Article

Photochemistry of Neutral Isonitrile Gold(I) Complexes: Modulation of Photoreactivity by Aurophilicity and π-Acceptance Ability

Oussama Elbjeirami, and Mohammad A. Omary

J. Am. Chem. Soc., **2007**, 129 (37), 11384-11393• DOI: 10.1021/ja0703933 • Publication Date (Web): 23 August 2007

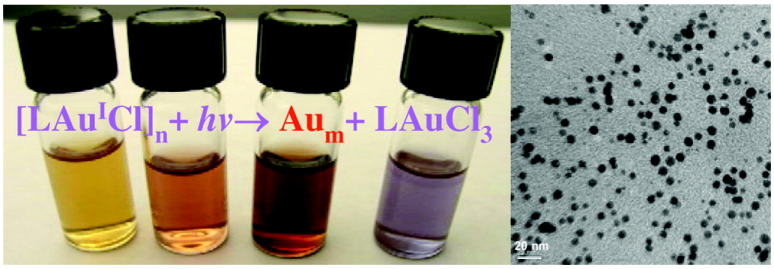

More About This Article

Additional resources and features associated with this article are available within the HTML version:

- Supporting Information
- Links to the 7 articles that cite this article, as of the time of this article download
- Access to high resolution figures
- Links to articles and content related to this article
- Copyright permission to reproduce figures and/or text from this article

View the Full Text HTML

J|A|C|S
ARTICLES
Published on Web 08/23/2007

Photochemistry of Neutral Isonitrile Gold(I) Complexes: Modulation of Photoreactivity by Aurophilicity and π-Acceptance Ability

Oussama Elbjeirami and Mohammad A. Omary*

Contribution from the Department of Chemistry, University of North Texas, Denton, Texas 76203

Received January 18, 2007; E-mail: omary@unt.edu

Abstract: This work demonstrates for the first time that aurophilicity and ligand π-acceptance ability sensitize the photoreactivity of Au(I) complexes. Photolysis of $LAu^{I}Cl$ (L = RNC or CO) complexes leads to free L, Au^{III}, and Au^{0} photoproducts. Solutions of (*p*-tosyl)$CH_2NCAuCl$ in dichloromethane undergo significant oligomerization leading to dimers and trimers with formation constants of 1.61×10^3 and 6.61×10^3 M^{-1}, respectively, representing the highest values reported to date for complexes that exhibit aurophilic association in solution. The photoproduct quantum yield (Φ) varies with the $LAu^{I}Cl$ concentration in solution. For (*p*-tosyl)$CH_2NCAuCl$, metallic gold forms with $\Phi = 0.0065$ and 0.032 in 4.0×10^{-5} and 4.0×10^{-3} M dichloromethane solutions, respectively. Meanwhile, irradiation of *t*-BuNCAuCl primarily produces *t*-$BuNCAuCl_3$ with $\Phi = 0.0045$ and 0.013 for 5.0×10^{-5} and 5.0×10^{-3} M dichloromethane solutions, respectively. For Au(CO)Cl, metallic gold forms with $\Phi = 0.013$ and 0.065 upon irradiation of 8.0×10^{-5} and 8.0×10^{-3} M dichloromethane solutions, respectively. Hence, $*[LAuX]_n$ oligomeric species are more photoreactive than monomeric species. The results also demonstrate intuitive control of Φ via modulation of the π-acceptance ability of L, as both follow CO > (*p*-tosyl)CH_2NC > (alkyl)NC in LAuCl, a trend that is also commensurate with the relative long-term photosensitivity of the corresponding solids and solutions. A new method for preparing stable small gold nanoparticles is described based on the fundamental findings above. Thus, photolysis of different concentrations of LAuX in solutions containing a primary amine-terminated dendrimer leads to clear solutions exhibiting tunable visible plasmon absorptions of gold nanoparticles; these solutions maintain their colors and stability indefinitely. TEM measurements for representative samples prepared by photolysis of (*p*-tosyl)$CH_2NCAuCl$ solutions give rise to spherical nanoparticles as small as 5 nm.

Introduction

Metal isonitriles have traditionally been strongly overshadowed by metal carbonyls, probably because of the repulsive scent of isonitriles and not necessarily due to scientific reasons.[1] Exploring the chemistry of metal isonitriles has led to new advances in both science and technology. For example, Cardiolite, which has been approved for use in cardiac imaging, is an isonitrile complex.[2] Gold(I) isonitrile complexes are used for the deposition of gold films[3,4] and preparation of new liquid crystalline phases.[5−7] Elegant work pioneered by Schmidbaur and co-workers has demonstrated fascinatingly diverse supramolecular structures exhibited by the Au(RNC)X class of compounds.[8] Thus, one can obtain dimers, larger oligomers, one-dimensional extended-chain polymers, or two-dimensional polymeric sheets by varying the R group and X.[8−19]

Gold(I) compounds can be active in homogeneous catalysis, overcoming previous problems associated with using Au(III) in catalysis due to its quick reduction to metallic gold.[20] The

(1) A recent paper has shown that fragrant isonitriles can actually be prepared; see: Pirrung, M. C.; Ghorai. S. *J. Am. Chem. Soc.* **2006**, *128*, 11772.
(2) Du Pont Merck Pharmac. Co. *Chem. Eng. News* **1991**, *Jan. 14*, 24.
(3) Norton, P. R.; Young, P. A.; Cheng, Q.; Dryden, N.; Puddephatt, R. J. *Surf. Sci*. **1994**, *307*, 172.
(4) Vaughan, L. G. U.S. Patent 3661959 19720509, 1972.
(5) Bachman, R. E.; Fioritto, M. S.; Fetics, S. K.; Cocker, T. M. *J. Am. Chem. Soc.* **2001**, *123*, 5376.
(6) Ishi, R.; Kaharu, T.; Pirio, N.; Zhang, S. W.; Takahashi, S. *J. Chem. Soc., Chem. Commun.* **1995**, *1215*.
(7) Kaharu, T.; Ishii, R.; Takahashi, S. *J. Chem. Soc., Chem. Commun.* **1994**, 1349.
(8) Schneider, W.; Angermaier, K.; Sladek, A.; Schmidbaur, H. *Z. Naturforsch. B* **1996**, *51*, 790.
(9) Mathieson, T. J.; Langdon, A. G.; Milestone, N. B.; Nicholson, B. K. *J. Chem. Soc., Dalton Trans.* **1999**, *201*.
(10) Bonati, F.; Minghetti, G. *Gazz. Chim. Ital.* **1973**, *103*, 373.
(11) Lentz, D.; Willemsen, S. *J. Organomet. Chem.* **2000**, *612*, 96.
(12) Eggleston, D. S.; Chodosh, D. F.; Webb, R. L.; Davis, L. L. *Acta Crystallogr.* **1986**, *C42*, 36.
(13) Ecken, H.; Olmstead, M. M.; Noll, B. C.; Attar, S.; Schlyer, B.; Balch, A. L. *J. Chem. Soc., Dalton Trans.* **1998**, 3715.
(14) Perreault, D.; Drouin, M.; Michel, A.; Harvey, P. D. *Inorg. Chem.1991, 30*, 2.
(15) Siemeling, U.; Rother, D.; Bruhn, C.; Fink, H.; Weidner, T.; Traeger, F.; Rothenberger, A.; Fenske, D.; Priebe, A.; Maurer, J.; Winter, R. *J. Am. Chem. Soc.* **2005**, *127*, 1102.
(16) Elbjeirami, O.; Omary, M. A.; Stender, M.; Balch, A. L. *Dalton Trans.* **2004**, 3173.
(17) White-Morris, R. L.; Olmstead, M. M.; Balch, A. L.; Elbjeirami, O.; Omary, M. A. *Inorg. Chem.* **2003**, *42*, 6741.
(18) Humphrey, S. M.; Mack, H. G.; Redshaw, C.; Elsegood, M. R. J.; Young, K. J. H.; Mayer, H. A.; Kaska, W. C. *Dalton Trans.* **2005**, 439.
(19) Schneider, D.; Schuster, O.; Schmidbaur, H. *Organometallics* **2005**, *24*, 3547.

10.1021/ja0703933 CCC: $37.00

photochemical deposition of metallic gold can be utilized for the fabrication of electronic devices.[21] Pioneering work by the Vogler group investigated Au(CO)Cl and showed that this complex exhibits a longest-wavelength absorption at $\lambda_{max} = 250$ nm that was assigned to a metal-centered *ds* transition.[22] The photolysis of Au(CO)Cl in CH_2Cl_2 leads to formation of AuCl and CO; the release of the latter is similar to photoreactions known for other metal carbonyl complexes in which ligand-field excitation leads to the population of M-L σ^* orbitals.[22] The initial photoproduct AuCl was proposed to disproportionate into metallic gold and gold(III) chloride.[22] The electronic structure of RNC is believed to be rather similar to that of CO; thus, the reactivities should be similar for complexes of both ligand types.[23] By analogy to the aforementioned Au(CO)Cl photochemical study, we have decided to investigate the compounds RNCAuCl (R = *t*-Bu, Me, (*p*-tosyl)CH_2). To the best of our knowledge, photochemical studies of isonitrile Au(I) complexes have never been reported prior to this effort.

Yersin and Gliemann demonstrated that the emissions of various $[Pt(CN)_4]^{2-}$ salts occur as a result of Pt···Pt extended-chain interactions in crystals.[24] It was suggested that association of such compounds might also occur in solution, thus affecting their photophysical behavior.[25] Related studies by Adamson and co-workers indeed demonstrated a non-Beer's law behavior of the electronic absorption spectral bands for aqueous solutions of $K_2Pt(CN)_4$ and $BaPt(CN)_4$ due to oligomerization in solution, which consequently affected the photophysical[26a] and photochemical[26b] behavior. In a similar fashion, Rh···Rh interactions in Rh(I) isocyanide complexes were shown to persist in solution with a non-Beer's law behavior of the electronic absorption spectral bands.[27] Another study by Pfab and Gerhardt demonstrated that even single crystals of the tetracyanoplatinates(II) exhibit photochemical activity (photooxidation).[28] Inspired by these studies for d^8 complexes, we have decided to investigate whether Au···Au interactions take place in solution and whether they influence the photochemistry of the Au(I) complexes studied herein. This is a particularly compelling study due to the significance of such interactions in Au(I) complexes, which have led to the "*aurophilic attraction*" concept originally coined by Schmidbaur.[29] This interaction type falls under the general category of "*metallophilic bonding*", which has been reviewed by Pyykko.[30,31] While multiple spectroscopic investigations have been carried out for isonitrile and carbonyl Au(I) complexes and illustrated the strong influence played by aurophilic bonding on the photophysical properties,[13−19,32] the present work represents the first study that examines the effect of aurophilicity on the photochemical reactivity of Au(I) complexes. In addition, we systematically examine the effect of the electronic factor on the photoproduct quantum yield in RNCAuCl and Au(CO)Cl complexes because the neutral ligands offer a range of σ-donation/π-acceptance ability.[23,33,34] We also report the utilization of these fundamental findings to prepare small gold nanoparticles stabilized in solutions of primary amine dendrimers. While gold is inert in its bulk form, size reduction to the nanoscale is known to lead to immense applications that range from catalysis and photonics to cancer imaging and therapy.[35,36] Common methods for preparing stable gold nanoparticles are based on chemical or electrochemical reduction[35,36] while, to our knowledge, this is the first example by which photochemistry of Au(I) complexes is used to prepare stable gold nanopatricles without using reducing agents.

Experimental Section

Materials and Syntheses. The preparations of RNCAuCl (R = (*p*-tosyl)CH_2, Me, and *t*-Bu) followed procedures reported previously.[12,16] The isonitriles (*p*-tosyl)CH_2NC and *t*-BuNC were purchased from ACROS Organics while Au(CO)Cl was purchased from Strem Chemicals. The dendrimer 16-cascade/1,4-diaminobutane[4-*N*,*N*,*N*′,*N*′]/(1-azabutylidyne)^2/aminopropane was purchased from Sigma-Aldrich under the commercial name "DAB-Am-16, Polypropylenimine hexadecaamine", G 3.0; henceforth we will refer to this dendrimer as "DAB-Am-16". Au(tetrahydrothiophene)Cl and MeNC were synthesized by slight modifications of published procedures.[37,38] HPLC grade solvents (acetonitrile, methanol, and dichloromethane) were distilled from conventional drying agents, degassed by the freeze−pump−thaw method three times prior to use, and kept under argon. All electronic absorption measurements were carried out under argon. Au(CO)Cl is light and moisture sensitive so the solution preparation was carried out in a glovebox and the samples were stored in the dark under argon. *CAUTION! Isonitrile compounds are toxic and need to be handled with adequate ventilation due to their stench; extra care should be taken to avoid contact with solids and solutions containing such compounds.*

Photolysis Reactions. Solutions of compounds studied photochemically were freshly prepared from dried CH_2Cl_2 under argon. A 5-mL or 25-mL aliquot of each solution was irradiated with UV light by using a Hanovia 450 W medium-pressure Hg lamp at ambient temperature with no heat detected. Changes in the electronic absorption spectra during the photolysis reactions were monitored using a Perkin-Elmer Lambda-900 double-beam UV/vis/NIR absorption spectrophotometer. HPLC data were collected using a Shimadzu SPD-6A spectrophotometer coupled with an LC-600 Shimadzu liquid chromatogram detector. A continuous flow of 0.5 mL/min was maintained using

(20) Teles, J. H.; Brode, S.; Chabanas, M. *Angew. Chem., Int. Ed.* **1998**, *37*, 1415.
(21) (a) D'Amico, J. F.; De Angelo, M. A.; Henrickson, J. F.; Kenney, J. T.; Sharp, D. J. *J. Electrochem. Soc.* **1970**, *118*, 1695. (b) D'Amico, J. F.; Litt, F. A.; De Angelo, M. A. *J. Electrochem. Soc.* **1972**, *119*, 256.
(22) (a) Kunkely, H.; Vogler. A. *J. Organomet. Chem.* **1997**, *541*, 177 (b) Vogler, A.; Kunkely, H. *Coord. Chem. Rev.* **2001**, *219*, 489.
(23) Malatesta, L.; Bonati, F. *Isocyanide Complexes of Metals*; Interscience: New York, 1969.
(24) For an example, see: (a) Yersin, H. *J. Chem. Phys.* 1**978**, *68*, 4707. For reviews, see: (b) Gliemann, G.; Yersin, H. *Struct. Bonding* **1985**, *62*, 87. (c) Yersin, H.; Gliemann, G. *Ann. N.Y. Acad. Sci.* **1978**, *313*, 539.
(25) Gliemann, G.; Lechner, A. *J. Am. Chem. Soc.* **1989**, *111*, 7469.
(26) (a) Schindler, J. W.; Fukuda, R. C.; Adamson, A. W. *J. Am. Chem. Soc.* **1982**, *104*, 3596. (b) Schindler, J. W.; Adamson, A. W. *Inorg. Chem.* **1982**, *21*, 4236.
(27) Mann. K. R.; Lewis, N. S.; Williams, R. M.; Gray, H. B.; Gordon, J. G., II. *Inorg. Chem.* **1978**, *17*, 828.
(28) Pfab, W. A.; Gerhardt, V. *J. Lumin.* **1984**, *31/32*, 582.
(29) Schmidbaur, H. *Chem. Soc. Rev.* **1995**, *24*, 391.
(30) Pyykkö, P. *Chem. Rev.* **1997**, *97*, 599.
(31) (a) Pyykkö, P. *Angew. Chem., Int Ed.* **2004**, *43*, 4412. (b) Pyykkö, P. *Inorg. Chim. Acta* **2005**, *358*, 4113.
(32) Elbjeirami, O.; Yockel, S; Campana, C. F.; Wilson, A. K.; Omary, M. A. *Organometallics* **2007**, *26*, 2550.
(33) Cotton. A. F.; Zingalez, F. *J. Am. Chem. Soc.* **1961**, *83*, 351.
(34) Csonka, I. P.; Szepes, L.; Modelli, A. *J. Mass Spectrom.* **2004**, *39*, 1456.
(35) For some representative examples, see: (a) Huang, X.; El-Sayed, I. H.; Qian, W.; El-Sayed, M. A. *J. Am. Chem. Soc.* **2006**, *128*, 2115. (b) Zheng, J.; Zhang, C.; Dickson, R. M. *Phys. Rev. Lett.* **2004**, *93*, 077402. (c) Li, J.; Li, X.; Zhai, H. J.; Wang, L. S. *Science* **2003**, *299*, 864. (d) Chen, S. W.; Ingram, R. S.; Hostetler, M. J.; Pietron, J. J.; Murray, R. W.; Schaaff, T. G.; Khoury, J. T.; Alvarez, M. M.; Whetten, R. L. *Science* **1998**, *280*, 2098. (e) Zheng, N,; Stucky, G. *J. Am. Chem. Soc.* **2006**, *128*, 14278. (f) An, Z.; Tang, W.; Hawker, C. J.; Stucky, G. *J. Am. Chem. Soc.* **2006**, *128*, 15054. (g) Goodman, D. W.; Chen, M. S. *Science* **2004**, *306*, 252. (h) Goodman, D. W.; Choudhary, T. V. *Appl. Catal.* **2005**, *291*, 32. (i) Loo, C.; Lowery, A.; Halas, N.; West, J.; Drezek, R. *Nano Lett.* **2005**, *5*, 709.
(36) For reviews, see: (a) El-Sayed, M. A. *Acc. Chem. Res.* **2001**, *34*, 257. (b) Kreibig, U.; Vollmer, M. *Optical Properties of Metal Clusters;* Springer-Verlag: Berlin, 1995.
(37) Usón, R.; Laguna, A. *Organometallic Syntheses*; King, R. B., Eisch, J. J., Eds.; Elsevier: Amsterdam, 1986.
(38) Schuster, R. E.; Scott, J. E.; Cazanova, J. *Org. Synth.* **1966**, *46*, 75.

Table 1. Deviation From Beer's Law in Dilute Solutions of (*p*-tosyl)CH_2NCAuCl and *t*-BuNCAuCl

(*p*-tosyl)CH_2NCAuCl		*t*-BuNCAuCl	
c_o, M	ϵ_{227}, M^{-1} cm^{-1}	c_o, M	ϵ_{230}, M^{-1} cm^{-1}
3.2×10^{-6}	3.5×10^4	2.3×10^{-6}	8.4×10^4
5.2×10^{-6}	7.2×10^3	3.8×10^{-6}	5.4×10^4
5.2×10^{-5}	4.4×10^3	3.8×10^{-5}	1.2×10^4
5.2×10^{-4}	1.3×10^3	3.8×10^{-4}	4.7×10^3

HPLC-grade methanol. The column used was Discovery C-18 (5 cm $\times$ 4.6 mm $\times$ 5 μm particle size).

Dendrimer-stabilized gold nanoparticles were prepared in a two-step process. First, a 1-mL aliquot of a 1×10^{-3} M solution of DAB-Am-16 in methanol was mixed with 4-mL solutions having different concentrations of (*p*-tosyl)CH_2NCAuCl in dichloromethane. Second, the resulting 5-mL solution was irradiated at ambient temperature with the aforementioned Hg lamp. After 1−2 h of exposure, the solutions were analyzed by electronic absorption spectroscopy. The morphology and size of the gold nanoparticles were determined via transmission electron microscopy (TEM) using a 200 kV high-resolution imaging TEM (JEOL 2100F). The solution of each sample was dispersed and dried on a carbon-coated Cu grid.

Results

Spectroscopic Studies. Dilute solutions of (*p*-tosyl)CH_2NCAuCl exhibit electronic absorption spectra with a major band at 225−227 nm ($\epsilon_{max} = 3.3 \times 10^4$ M^{-1} cm^{-1} in acetonitrile) assignable to charge-transfer transitions in monomeric molecules.[32,39] Similarly, dilute solutions of *t*-BuNCAuCl and MeNCAuCl exhibit electronic absorption spectra with major bands around 230−240 nm ($\epsilon_{max} = 8.4 \times 10^4$ and 3.2×10^4 M^{-1} cm^{-1} in acetonitrile, respectively). The effective chromophore in the three complexes is the C−N≡C−Au^ICl unit while slight absorption changes are expected upon varying the R group on the ligand. On the other hand, dilute solutions of Au(CO)Cl in acetonitrile exhibit electronic absorption spectra with major bands in the 208−222 nm range ($\epsilon_{max} = 1.95 \times 10^4$ M^{-1} cm^{-1}), similar to the absorption data reported by Kunkely and Vogler for this compound.[22] The effect of association of Au(CO)Cl on the absorption and luminescence of this compound in solution and the solid state has been addressed in an experimental/theoretical study that we have recently reported,[32] whereas in the work herein we examine the solution association for RNCAuCl complexes.

Intermolecular interactions lead to deviations from Beer's law. Table 1 shows some representative data for the neutral isonitrile complexes studied herein and illustrates a clear negative deviation from Beer's law for the monomer bands. This is not due to real limitations of Beer's law, which are normally encountered when the analyte concentration is 0.01 M or higher,[40] whereas we observe the negative deviation at much lower concentrations (Table 1). Thus, we attribute the deviation from Beer's law in this study to oligomerization of monomeric RNCAuCl complexes, for which aurophilic bonding in solution is at least one contributing factor in addition to other possible intermolecular forces such as multipolar interactions.[41,17]

The oligomerization process for LAu^ICl complexes can be represented by eq 1, with a monomer-"*n*-mer" equilibrium

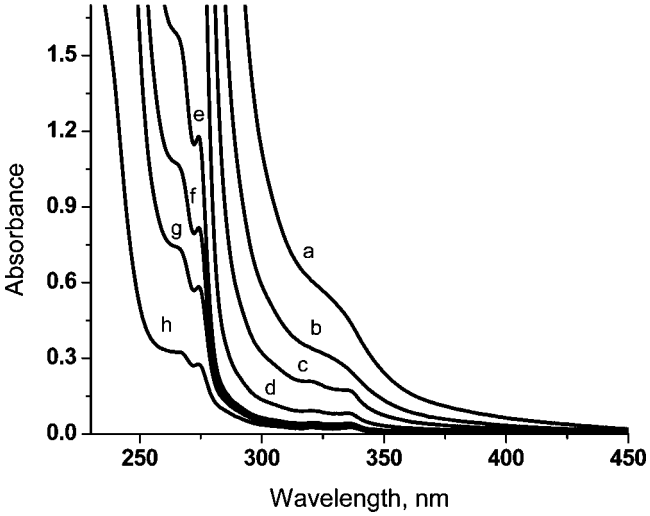

Figure 1. Electronic absorption spectra vs concentration of (*p*-tosyl)CH_2NCAuCl in dichloromethane at room temperature using a 1-cm cuvette. The total (*p*-tosyl)CH_2NCAuCl concentration is (a) 0.0468 M, (b) 0.0234 M, (c) 0.0156 M, (d) 0.009 36 M, (e) 0.006 68 M, (f) 0.005 85 M, (g) 0.005 21 M, and (h) 5.21×10^{-4} M.

constant given by eq 2, wherein c_1 and c_n represent the concentration of the monomer and *n*-mer, respectively.

$$n[LAu^ICl] \rightleftarrows [LAu^ICl]_n \quad (1)$$

$$K_{1n} = c_n/c_1^n \quad (2)$$

At higher concetrations, the tendency for oligomer formation increases. This is evident by the appearance of lower-energy absorption bands (e.g., at 275, 320, and 335 nm for (*p*-tosyl)CH_2NCAuCl; see Figure 1). Assuming that the peak at 275 nm is due to an oligomer, a general quantitative formula that describes the equilibrium shown in eq 2 can be derived as eq 3,[26a,27,42] wherein c_o is the initial concentration of (*p*-tosyl)CH_2NCAuCl, A is the maximum absorbance, ϵ_n is the molar absortiviy of the *n*-mer, and b is the light path.

$$c_o A^{-1/n} = (n/\{\epsilon_n b\})A^{(n-1)/n} + (K_{1n}\epsilon_n b)^{-1/n} \quad (3)$$

A reasonable fit ($R^2 = 0.999$) is obtained by plotting $c_o A^{-1/2}$ vs $A^{1/2}$ (Figure 2a), therefore suggesting that the peak at 275 nm is due to a [(*p*-tosyl)CH_2NCAuCl]$_2$ dimer. A value of (1.61 $\pm$ 0.34) $\times$ 10^3 M^{-1} is obtained for the formation constant of the dimer, K_{12}, at ambient temperature. The oligomer responsible for the 320 and 335 nm bands is determined to correspond to a trimer according to our quantitative analysis. These trimer bands grow along with the dimer band at 275 nm but with a different concentration dependence. In the determination of K_{13}, we have subtracted the concentration of the dimer (using the derived value of K_{12}) from the initial concentration of (*p*-tosyl)CH_2NCAuCl.[42] Using the corrected c_o, plotting $c_o A^{-1/3}$ vs $A^{2/3}$ (Figure 2b) gives a linear equation with a reasonable fit ($R^2 =$ 0.997). A value of (6.61 $\pm$ 0.40) $\times$ 10^3 M^{-1} for the formation constant of the trimer, K_{13}, is obtained at ambient temperature. We obtain further thermodynamic parameters for the solution association by carrying out these measurements versus temperature. Thus, Table 2 summarizes the formation constants, molar

(39) Chastain, S. K.; Mason, W. R. *Inorg. Chem.* ***1982***, *21*, 3717.
(40) Skoog, D. A.; Holler, F. J.; Nieman, T. A. *Principles of Instrumental Analysis*, 5th ed.; Harcourt Brace: Philadelphia, 1998.
(41) Liau, R.-Y.; Mathieson, T.; Schier, A.; Berger, R. J.; Runeberg, N.; Schmidbaur, H. *Z. Naturforsch. B* **2002**, *57*, 881.
(42) Rawashdeh-Omary, M. A.; Omary, M. A.; Patterson, H. H. *J. Am. Chem. Soc.* **2000**, *122*, 10371.

Table 2. A Summary of the Formation Constants, Molar Absorptivities, Free Energies, Enthalpies, and Entropies for the Formation of a [(*p*-tosyl)$CH_2NCAuCl]_2$ Dimer (λ_{max} = 275 nm) and a [(*p*-tosyl)$CH_2NCAuCl]_3$ Trimer (λ_{max} = 320 nm) in Solution

	ϵ_n, M^{-1} cm^{-1}	K_{1n}	ΔG_{1n} (298 K), kJ/mol	ΔH_{1n} (298 K), kJ/mol	ΔS_{1n} (298 K), J/K–mol
dimer	176 ± 5	$(1.61 \pm 0.34) \times 10^3$ M^{-1}	-18.3 ± 0.5	-28.6 ± 2.0	-34.9 ± 0.7
trimer	56.1 ± 2.0	$(6.61 \pm 0.40) \times 10^3$ M^{-2}	-21.8 ± 0.2	-36.5 ± 0.8	-49.5 ± 0.3

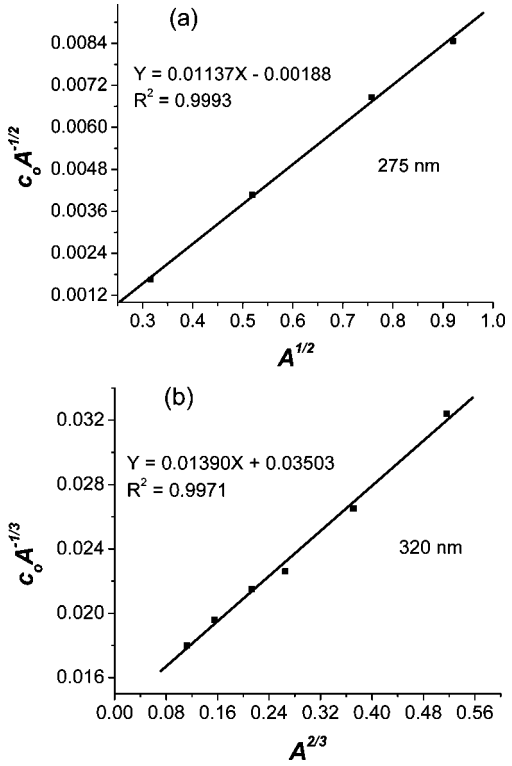

Figure 2. (a) A plot of $c_oA^{-1/2}$ vs $A^{1/2}$ with absorbance values taken at 275 nm, characteristics of a [(*p*-tosyl)$CH_2NCAuCl]_2$ dimer. (b) A plot of $c_oA^{-1/3}$ vs $A^{2/3}$ with absorbance values taken at 320 nm, characteristics of a [(*p*-tosyl)$CH_2NCAuCl]_3$ trimer. Absorption data in both plots have been taken at ambient temperature.

absorptivities, free energies, enthalpies, and entropies for the formation of [(*p*-tosyl)$CH_2NCAuCl]_2$ and [(*p*-tosyl)$CH_2NCAuCl]_3$ oligomers in solution.

Photochemistry of (*p*-tosyl)$CH_2NCAuCl$. Irradiation of dichloromethane solutions of this complex leads to photolysis that proceeds slowly, as indicated by the spectral changes for a 4.0×10^{-3} M solution after the first few exposure periods (Figure 3). The major near-UV band with λ_{max} = 320−350 nm and the weaker shoulder that extends to the visible region (∼440−470 nm) are signatures of charge transfer and ligand field transitions, respectively, for square-planar Au(III) complexes that contain chloride ligands ($AuCl_4^-$, Au_2Cl_6, or $LAuCl_3$).[43,44] The dominant molecular form of the square-planar Au(III) species in the photoproducts here is likely $RNCAu^{III}Cl_3$ in equilibrium with the free ligand and other Au(III) forms; see the Discussion section. The free (*p*-tosyl)CH_2NC ligand has an absorption band at ∼340 nm (see Figure S1 in the Supporting Information). Although its energy coincides with the absorptions of the photoprouncts, this band is too weak (ϵ = 8.70 M^{-1} cm^{-1}) to deduce the presence of the free ligand in equilibrium with an Au(III) complex based on absorption changes during photolysis of (*p*-tosyl)$CH_2NCAuCl$ solutions. However, evidence of photodissociation of the free (*p*-tosyl)CH_2NC ligand has been obtained by HPLC measurements. Thus, HPLC chromatograms for solutions of (*p*-tosyl)$CH_2NCAuCl$ show no peaks before photolysis while the photoproducts exhibit a peak with a retention time of 3.76 min. This peak is consistent with the free isonitrile ligand because a separate measurement for (*p*-tosyl)CH_2NC shows one peak with a retention time of 3.80 min; see Figure S2 in the Supporting Information.

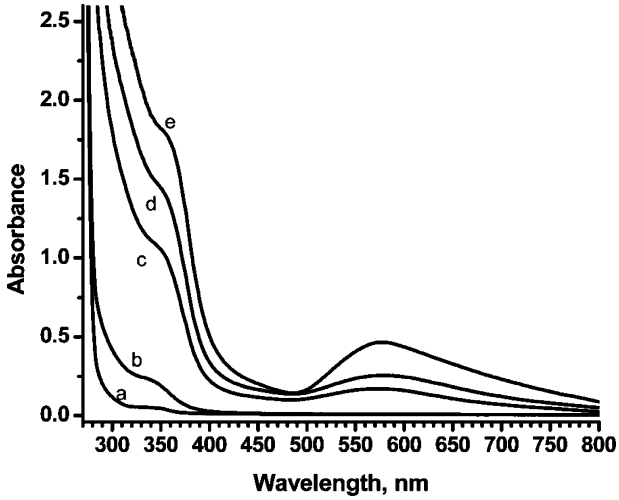

Figure 3. Absorption spectral changes during the photolysis of a 4.0×10^{-3} M solution of (*p*-tosyl)$CH_2NCAuCl$ in dichloromethane under argon at room temperature using a 1-cm cuvette after (a) 0, (b) 3, (c) 10, (d) 16, and (e) 30 min of irradiation with a 450-W Hg lamp.

Table 3. A Summary of the Photoproduct Quantum Yields $\Phi(Au^0)$ and $\Phi(LAuCl_3)$ vs Concentrations of (*p*-tosyl)$CH_2NCAuCl$, *t*-BuNCAuCl, MeNCAuCl, and Au(CO)Cl

	c_0, M	$\Phi(Au^0)$	$\Phi(LAuCl_3)$
(*p*-tosyl)$CH_2NCAuCl$	4.0×10^{-3}	0.032	N/A
	4.0×10^{-5}	0.0065	N/A
t-BuNCAuCl	5.0×10^{-3}	0.0087	0.013
	5.0×10^{-5}	0.0021	0.0045
MeNCAuCl	5.0×10^{-3}	N/A	0.0013
	5.0×10^{-5}	N/A	N/A
Au(CO)Cl	8.0×10^{-3}	0.065	0.041
	8.0×10^{-5}	0.013	0.0088

Analysis of the photolysis data in Figure 3 gives rise to Φ = 0.056 for the formation of (*p*-tosyl)$CH_2NCAuCl_3$. The solution color becomes darker upon continued irradiation, giving rise to broad peaks with λ_{max} ∼585 nm. These peaks are attributed to plasmon absorptions of colloidal gold particles, which form with Φ = 0.032. The increase in the baseline absorbance is a known consequence of the production of metallic gold particles.[22,43] Disproportionation of $[Au^ICl]_n$ species to form $Au^{III}$and Au^0 products is proposed as a secondary reaction governed by the thermodynamic instability[22,43] of $[Au^ICl]_n$ following photodissociation of the donor ligand. A 4.0×10^{-5} M solution exhibits a similar photochemical behavior with a very low efficiency (Φ = 0.0065 for metallic gold, Table 3).

(43) Puddephatt, R. J. *The Chemistry of Gold*; Elsevier: New York, 1978.
(44) (a) Gangopadhayay, A. K.; Chakravorty, A. *J. Chem. Phys* **1961**, *35*, 2206. (b) Potts, R. A. *J. Inorg. Nucl. Chem.* **1972**, *34*, 1749. (c) Nalbandia, L.; Boghosian, S.; Papatheodorou, G. N. *Inorg. Chem.* **1992**, *31*, 1769.

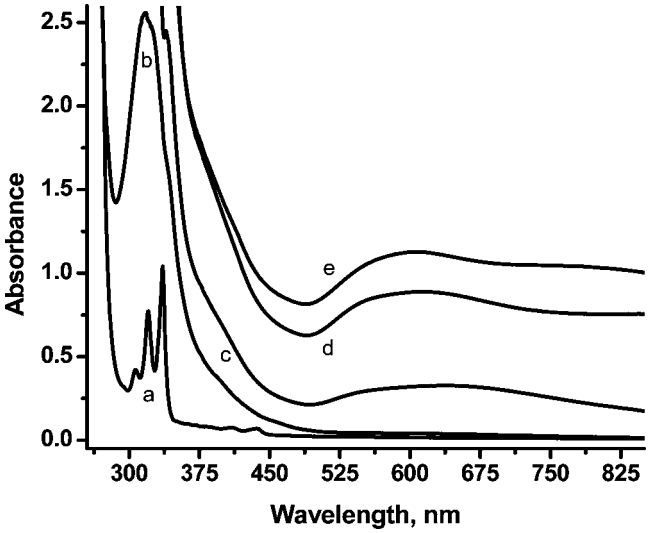

Figure 4. Absorption spectral changes during the photolysis of a 5.0×10^{-3} M solution of *t*-BuNCAuCl in dichloromethane under argon at room temperature using a 10-cm cuvette after (a) 0, (b) 11, (c) 35, (d) 80, and (e) 125 min of irradiation with a 450-W Hg lamp.

Photochemistry of RNCAuCl (R = *t*-Bu and Me). Figure 4 shows photolysis results for a 5.0×10^{-3} M solution of *t*-BuNCAuCl in dichloromethane. The solution exhibits slow photooxidation after several light exposure periods as indicated by the formation of a new band with λ_{max} near 325 nm attributed to *t*-BuNCAuCl$_3$, which forms with $\Phi = 0.013$. This absorption is sufficiently strong so as to mask the weak structured absorption of the complex before irradiation, which likely represents an $S_0 \rightarrow T_1$ monomer transition due its low extinction coefficient (20.8 M^{-1} cm^{-1}) and negative deviation from Beer's law ($\epsilon_{336.0}$ decreases to 7.3 M^{-1} cm^{-1} for a 9.0×10^{-3} M solution). With continued irradiation, the solution color becomes darker due to formation of colloidal gold particles with $\lambda_{max} =$ 602 nm and a calculated $\Phi = 0.0087$. In acetonitrile, the reaction is less efficient since the solvent can coordinate to stabilize the AuCl transient species before it can disproportionate. At a lower concentration (5.0×10^{-5} M) in dichloromethane, photolysis proceeds with a lower efficiency, affording metallic gold and *t*-BuNCAuCl$_3$ with $\Phi = 0.0021$ and 0.0045, respectively. The results suggest a smaller size for the gold nanoparticles formed from this solution based on the value of λ_{max} (565 nm compared to 602 nm for the 5.0×10^{-3} M solution) since gold nanoparticles are known to exhibit size-dependent absorption maxima.[45] HPLC data for a solution of the photoproducts shows only one peak with a retention time of 3.57 min. This peak is assigned to the free isonitrile ligand because an independent measurement for a solution of the free *t*-BuNC ligand in dichloromethane shows one peak with a retention time of 3.58 min.

The efficiency of the photolysis of MeNCAuCl in dichloromethane to give metallic gold is very low (the lowest among all compounds studied here) with MeNCAuCl$_3$ forming as the dominant photoproduct. After several exposures of a 5.0×10^{-3} M solution, photooxidation takes place for the Au(I) complex as suggested by the appearance of the band at $\lambda_{max} = 322$ nm due to MeNCAuCl$_3$, which remains the dominant feature even at longer exposure periods (Figure 5) but the efficiency is rather low, $\Phi = 0.0013$. Metallic gold does not form efficiently as this photoproduct can be obtained only after extended irradiation (8 h or longer).

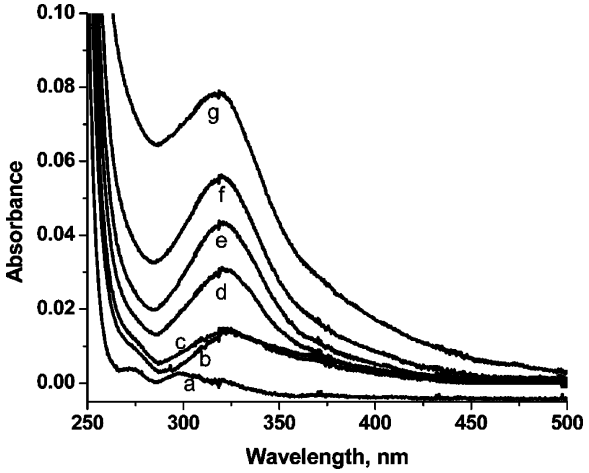

Figure 5. Absorption spectral changes during the photolysis of a 5.0×10^{-3} M solution of MeNCAuCl in dichloromethane under argon at room temperature using a 1-cm cuvette after (a) 0, (b) 2, (c) 5, (d) 10, (e) 15, (f) 25, and (g) 40 min of irradiation with a 450-W Hg lamp.

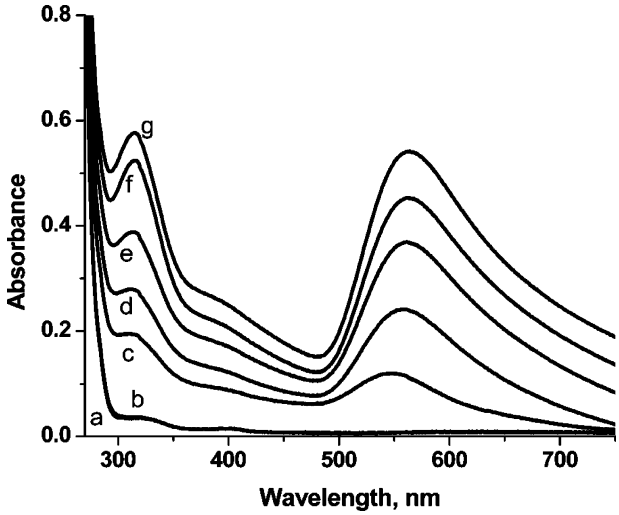

Figure 6. Absorption spectral changes during the photolysis of a 8.0×10^{-3} M solution of Au(CO)Cl in dichloromethane under argon at room temperature using a 1-cm cuvette after (a) 0, (b) 1, (c) 2.5, (d) 4, (e) 5.5, (f) 7, and (g) 9 min of irradiation with a 450-W Hg lamp.

Photochemistry of Au(CO)Cl vs Concentration. Photolysis data for a 8.0×10^{-3} M dichloromethane solution of Au(CO)Cl are shown in Figure 6. After several exposure periods, a new band appears at $\lambda_{max} = 318$ nm attributed to square-planar Au(III) photoproduct species, which form with $\Phi = 0.041$. This is accompanied by a darker solution associated with a visible band ascribed to colloidal gold ($\lambda_{max} = 565$ nm; $\Phi = 0.065$). At a lower concentration (8.0×10^{-5} M), the dominant feature is metallic gold ($\lambda_{max} = 552$ nm; $\Phi = 0.013$) but a weaker band assigned to Au(III) photoproducts also appears ($\lambda_{max} =$ 316 nm; $\Phi = 0.0088$). At a higher concentration of Au(CO)Cl, the photoreaction is more efficient, as indicated by the higher photoproduct quantum yield. It is worth mentioning that we have been able to reproduce the photochemical results of Kunkely and Vogler[22] for a 1.0×10^{-3} M solution of the Au(CO)Cl complex in dichloromethane since we obtain $\Phi = 0.019$ for the Au(III) photoproduct of this solution. This value is

(45) Fendler, J. H. *Nanoparticles and Nanostructured Films*; Wiley-VCH: Weinheim, 1998.

intermediate between those for the two solutions above so it serves to verify the trend of the concentration dependence of the photolysis quantum yield in addition to showing that the above values are not due to variation in experimental conditions between two laboratories. The efficiency of the photochemical process for Au(CO)Cl is higher than that for the RNCAuCl analogues. Table 3 compares the photochemical quantum yields for the RNCAuCl compounds with those for Au(CO)Cl at different concentrations.

Discussion

Aurophilic Bonding in Solution. Deviations from Beer's law have been studied for other d^{10} and d^8 closed-shell systems. Schindler and co-workers reported a negative deviation for a monomer MLCT band in aqueous solutions of $[Pt(CN)_4]^{2-}$, which was attributed to the formation of oligomers (trimers),[26] while Gray and co-workers reported a similar study for Rh(I)−isocyanide complexes.[27] As for d^{10} systems, Patterson and co-workers reported the association of $[Au(CN)_2]^-$ and $[Ag(CN)_2]^-$ complexes in water and methanol, in which negative deviations from Beer's law were attributed to the formation of dimers and trimers,[42] while Lin and co-workers reported another study for the association of dinuclear diphosphine−dithiolate Au(I) complexes in acetonitrile.[46] The ΔG_{12} value of −18.29 kJ/mol for the $[(p\text{-tosyl})CH_2NCAuCl]_2$ dimer at ambient temperature is higher than the reported values for both the mononuclear $[Au(CN)_2^-]_2$ complexes ($\Delta G_{12} = -7.08$ kJ/mol)[42] and dinuclear Au(diphosphine)(dithiolate) complexes (ΔG_{12} varied between −8.9 kJ/mol to −12 kJ/mol depending on the bridging ligands).[46] The higher value of the dimer formation constant and the corresponding more negative ΔG_{12} value for $[(p\text{-tosyl})CH_2NCAuCl]_2$ than these literature precedents suggest a thermodynamically stronger association in solutions of this neutral isonitrile compound (and perhaps stronger Au···Au aurophilic bonds; vide infra). The negative ΔS values for the dimer and the trimer of the $(p\text{-tosyl})CH_2NCAuCl$ complex are consistent with an association process and are comparable to those reported earlier by Lin and co-workers.[46] The extent of aurophilic bonding and other intermolecular interactions that contribute to the association of LAuCl complexes (L = CO or RNC) in solution affect the photochemical behavior and photoproduct quantum yields.

It is interesting that the absorption spectral data suggest that the association of $(p\text{-tosyl})CH_2NCAuCl$ in dichloromethane is not limited to dimer formation as trimers also form at high enough concentrations. This is particularly intriguing because crystals of $(p\text{-tosyl})CH_2NCAuCl$ have the molecules associating as crossed dimers in the solid state.[17] This result adds to rare literature precedents of greater association in solution than in the solid state for other d^{10} complexes. For example, Eisenberg and co-workers reported that solvent-free colorless crystals of a dimeric gold(I) dithiocarbamate complex are not emissive and do not exhibit Au···Au intermolecular interactions; yet, dissolving these crystals leads to fluid or glassy solutions that exhibit visible color and bright luminescence indicative of association of the molecules in solution.[47] Patterson and co-workers reported that increasing the concentration of dicyano Au(I) and Ag(I) complexes in aqueous solution progressively red-shifts their excitation band energies from those for dilute solutions, ultimately leading to excitation energies that are even lower than values for the corresponding solids.[42] Balch and co-workers reported a remarkable variation in the emission color of the Au(I) diaminocarbene complex $[Au\{C(NHMe)_2\}_2](PF_6)$ in frozen solutions of different solvents, several of which exhibited significantly red-shifted emissions from those for crystals.[48] The association of $(p\text{-tosyl})CH_2NCAuCl$ is driven by aurophilic bonding in the solid state and most likely also in solution. Crystals grown from dichloromethane solutions of this compound form a crossed-dimer structure with a nearly staggered conformation (in which aurophilic bonding plays the major stabilizing factor vs other intermolecular interactions).[16] The high formation constants and association free energies and enthalpies (Table 2) are consistent with staggered oligomers in solution, as the alternative parallel or antiparallel association modes are known to lead to lower stabilization energies (and longer aurophilic distances).[8,16,17,41,42]

Photolysis of RNCAuCl vs Au(CO)Cl. The electronic structure of gold(I) complexes with σ-donor/π-acceptor ligands (e.g., CO, CN^-) is strongly influenced by π back-bonding. Isocyanides are believed to be better σ-donors and poorer π-acceptors than carbonyl.[49,50] The nature of the R group can affect the degree of π-acceptance capability in the RNC family. An electron-withdrawing moiety (such as aryl-SO_2 in $(p\text{-tosyl})CH_2NC$) renders the isonitrile a better π-acceptor. On the other hand, electron-donating groups make the isonitriles better σ-donors and weaker π-acceptors, which is the situation in MeNC and *t*-BuNC in comparison with $(p\text{-tosyl})CH_2NC$. Johnston and Cooper have shown that the π-acceptance ability of substituted aryl isonitriles increases in the order *o*- or *p*-$CH_3OC_6H_4NC$ < *o*- or *p*-$CH_3C_6H_4NC$ < C_6H_5NC < *o*- or *p*-FC_6H_4NC < *o*- or *p*-$CF_3C_6H_4NC$ < *o*- or *p*-ClC_6H_4NC < *o*- or *p*-$NO_2C_6H_4NC$, while the σ-donation ability follows the opposite order.[51] Chemical intuition suggests that the stronger the π acceptance ability in organometallic LAuX complexes, the higher the absorption energy, the greater the M−C bonding character of the originating filled orbital depopulated, and the greater the M−C antibonding character in the destination virtual orbital populated. This suggested model is shown in Figure 7. The spectral and photochemical data herein suggest that this model is borne out. The relative absorption energies for dilute solutions that represent monomer forms of the complexes in this study before irradiation are consistent with this model. Thus, dilute solutions of Au(CO)Cl in acetonitrile exhibit absorption bands at $\lambda_{max} = 207$ and 220 nm, which are blue-shifted from the major absorption band at $\lambda_{max} = 227$ nm for analogous solutions of $(p\text{-tosyl})CH_2NCAuCl$, which in turn is blue-shifted from the 230−240 nm bands exhibited by analogous solutions of *t*-BuNCAuCl and MeNCAuCl. Consequently, the observed experimental λ_{max} values for the LAuX complexes examined herein support our intuitive premise that stronger π-acceptor

(46) Tang, S. S.; Chang, C. P.; Lin, I. J. B.; Liou, L. S.; Wang, J. C. *Inorg. Chem.* **1997**, *36*, 2294.
(47) Mansour, M. A.; Connick, W. B.; Lachicotte, R. J.; Gysling, H. J.; Eisenberg, R. *J. Am. Chem. Soc.* **1998**, *120*, 1329.
(48) White-Morris, R. L.; Olmstead, M. M.; Jiang, F.; Tinti, D. S.; Balch, A. L. *J. Am. Chem. Soc.* **2002**, *124*, 2327.
(49) Elschenbroich, C.; Salzer, A. *Organometallics: A Concise Introduction*, 2nd ed.; VCH: Weinheim, 1992.
(50) Mathieson, T.; Schier, A.; Schmidbaur, H. *J. Chem. Soc., Dalton Trans.* **2001**, *1196*.
(51) Johnston, R. F.; Cooper, J. C. *J. Mol. Struct.* **1991**, *236*, 297.

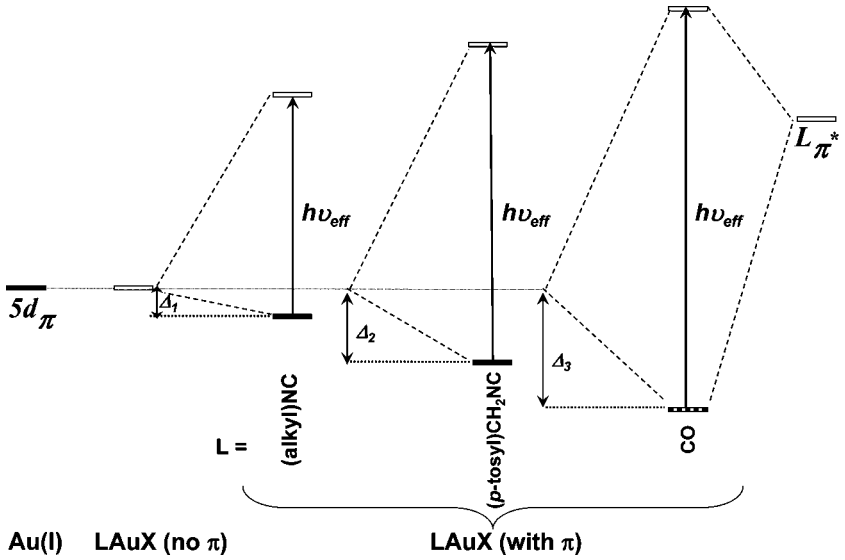

Figure 7. A model for the frontier orbitals showing the effective transition that leads to photolysis upon modulation of the π-acceptance ability of the L ligand in LAuX complexes. The Δ parameter represents the extent of π acceptance since it shows the deviation from the nonbonding character of the $5d_\pi$ orbitals of Au(I) predicted by the σ-only bonding scheme of the crystal-field theory.

ligands will have a higher absorption energy due to the increasing Δ parameter shown in the model suggested in Figure 7.

The effective absorption that leads to photolysis entails removing an electron from $5d_\pi$ orbitals, which are nonbonding in the σ-bonding scheme according to simple crystal-field theory concepts. However, when π bonding is considered, an increase in the π-acceptance ability of the L ligand in LAuX leads to a greater M−C bonding character in the $5d_\pi$ orbitals and greater M−C antibonding character in the neutral ligand's π^* orbitals. Hence, depopulation of the bonding $5d_\pi$ orbitals and population of the ligand π^* orbitals on exposure of the linear LAuCl complex to a broad-band UV light lead to dissociation of L ligands with an efficiency that should increase on going from L = (alkyl)NC → (*p*-tosyl)CH_2NC → CO since the π-acceptance ability increases in the same direction. This is exactly the trend of the quantum yield values we observe for these complexes, as summarized in Table 3. The model suggested in Figure 7 is different from the one proposed by Kunkely and Vogler for the Au(CO)Cl complex, which suggested that the photolysis is caused by the weak "*ds*" absorption transition that populates the Au(I) 6*s* orbital, arguing that the latter orbital is destabilized by σ-interaction with the ligands in a similar manner to that for the destabilization of the e_g^* ligand-field orbitals in octahedral metal carbonyls.[22] These authors suggested that, albeit weak, the "*ds*" transition has a larger effect on the Au−CO bonding than the much stronger higher-energy major absorption bands that were assigned as "*dp*" or "MLCT" in ref 22. Adopting the model in ref 22 would lead to an opposite trend of the relative quantum yields in this study since the RNC ligands are stronger σ-donors and weaker π-acceptors than CO.

We now turn our attention to explaining the increased photoreactivity upon increasing the concentration of the neutral complexes. As dimers and higher oligomers form in more concentrated solutions, aurophilic bonding red-shifts the absorption energies of the effective photolysis transitions and thus lower-energy photons will also contribute to the photolysis reactions along with the higher-energy photons that excite both the monomers and oligomers. Consequently, higher photoproduct quantum efficiency will be obtained at higher concentrations versus dilute solutions. Balzani and co-workers have reported that dilute (10^{-2}−10^{-4} M) aqueous solutions of $[Pt(CN)_4]^{2-}$ show no photochemistry to 254-nm irradiation.[52] However, subsequent studies by Adamson and co-workers showed that the triplet excited states of the oligomers present at high concentrations of $[Pt(CN)_4]^{2-}$ are photoreactive by a two-electron oxidation pathway in the presence of a good two-electron oxidant.[26b] Later on, Pfab and Gerhardt demonstrated that Pt^{II} chains in solid tetracyanoplatinates(II) exhibit photochemical activity as a result of removing an electron from the one-dimensional valence band and placing it into a lattice site between chains, which are octahedrally coordinated by water molecules that act as acceptors.[28] We are unaware of literature precedents for concentration-dependent photolysis studies of d^{10} complexes, but there is precedence for concentration-dependent studies of reagents added to such complexes to sensitize their photoreactivity. For example, Kunkely and Vogler observed higher photolysis quantum yields for $AuCl_2^-$ and $AuBr_2^-$ in the presence of higher concentrations of electron acceptors such as CH_2Cl_2 or O_2 but not the Au(I) complex itself.[53]

Despite the fact that all LAuX complexes herein (L = RNC or CO) exhibit higher photolysis quantum yields at higher concentrations, the electronic factor (π acceptance ability of L) distinguishes them better from one another in regards to photoreactivity. The difference among the compounds in the supramolecular association mode in their crystalline solid state does not seem to have any bearing on the trends of the quantum yields, although this is the major factor that governs their solid-state luminescence behavior.[16,32] The solid-state association mode for the most photoreactive Au(CO)Cl and least photoreactive (alkyl)NCAuCl compounds is the same (antiparallel chains), while the photoreactivity was intermediate for the (*p*-tosyl)CH_2NCAuCl compound whose crystals exhibit a crossed-dimer structure.

(52) Moggi, L.; Bolletta, F.; Balzani, V.; Scandola, F. *J. Inorg. Nucl. Chem.* **1966**, *28*, 2589.
(53) Kunkely, H.; Vogler, A. *Inorg. Chem.* **1992**, 31, 4539.

We propose that the photolysis of $LAu^{I}Cl$ (L = CO and RNC) in solution will lead to the following photochemical reaction scheme upon absorbing UV irradiation, with the efficiency of each step and the "*n*" value depending on the concentration and extent of oligomerization:

$$[LAu^{I}Cl]_n + h\nu \rightarrow {}^*[LAu^{I}Cl]_n \quad \textit{(Photoexcitation)} \quad \text{(i)}$$

$${}^*[LAu^{I}Cl]_n \rightarrow L + [Au^{I}Cl]_n \quad \textit{(Photodissociation)} \quad \text{(ii)}$$

$$[Au^{I}Cl]_n + L \rightarrow Au^0 + LAu^{III}Cl_3 \quad \textit{(Disproportionation)} \quad \text{(iii)}$$

$$m\,Au^0 \rightarrow Au_m{}^0 \quad \textit{(Nanoparticle formation)} \quad \text{(iv)}$$

$$[LAu^{I}Cl]_n + h\nu \rightarrow Au_m{}^0 + LAu^{III}Cl_3 \quad \textit{(Overall reaction)}$$

This mechanism provides an explanation for the sensitivity of the photochemical reactivity to concentration (hence aurophilicity) of the LAuX complex because the proposed reactive species is an oligomer. Nevertheless, additional processes likely compete with or complement the proposed mechanism. For example, direct oxidation or reduction without necessarily going through the intermediate AuCl may be possible. Solvent-initiated photoreactions are particularly relevant in halogenated solvents, and it is often difficult to distinguish such processes from metal-centered photoreactions.[54] A solvent-initiated photoreaction may lead to oxidation of $RNCAu^{I}Cl$ to form $RNCAu^{III}Cl_3$ and $H[AuCl_4]$ in a manner akin to that suggested by Serafimova and Hoggard for $Au(PPh_3)Cl$.[54b] Although this mechanism does not account for the formation of Au nanoparticles, it cannot be completely ruled out because we observe some variation in the distribution of the photoproducts upon changing the neutral ligand in the different LAuCl complexes studied here. For example, photolysis of MeNCAuCl does not attain Au nanoparticles while other complexes do to different extents (see Figures 3−6 and Table 3).

Among the multiple reasonable possibilities for the exact molecular form of the Au(III) complex in the photoproducts, we adopt an assignment to square-planar $LAu^{III}Cl_3$ complexes although it is likely that this species is in equilibrium with the free ligand and other Au(III) forms. The presence of the free ligand in the photoproduct mixture is substantiated by HPLC data (vide supra). The Au(III) species are likely aggregated and/or solvated to form molecular units such as Au_2Cl_6, $LAuCl_3$, $(Sol)AuCl_3$, and $H[AuCl_4]$ (L = neutral ligand, Sol = solvent molecule). The absorption spectral changes in this work and in similar photochemical studies reported for Au(I) complexes[22,53−55] are insufficient to identify the exact identity of these Au(III) species because they have rather similar absorption profiles.[43,44,54] Because of some variation in peak maxima with different ligands, we prefer the assignment to $LAuCl_3$ although some of the other aforementioned forms as well as the free ligand are likely present. The Au_2Cl_6 form may exist as a result of disproportionation of AuCl species before diffusion of and collision with the photodissociated ligand. The $H[AuCl_4]$ form is possible in the solvent-initiated competing mechanism, as discussed above, while the $(Sol)AuCl_3$ form is particularly relevant with ligating solvents such as acetonitrile (but even dichloromethane is not completely innocent).

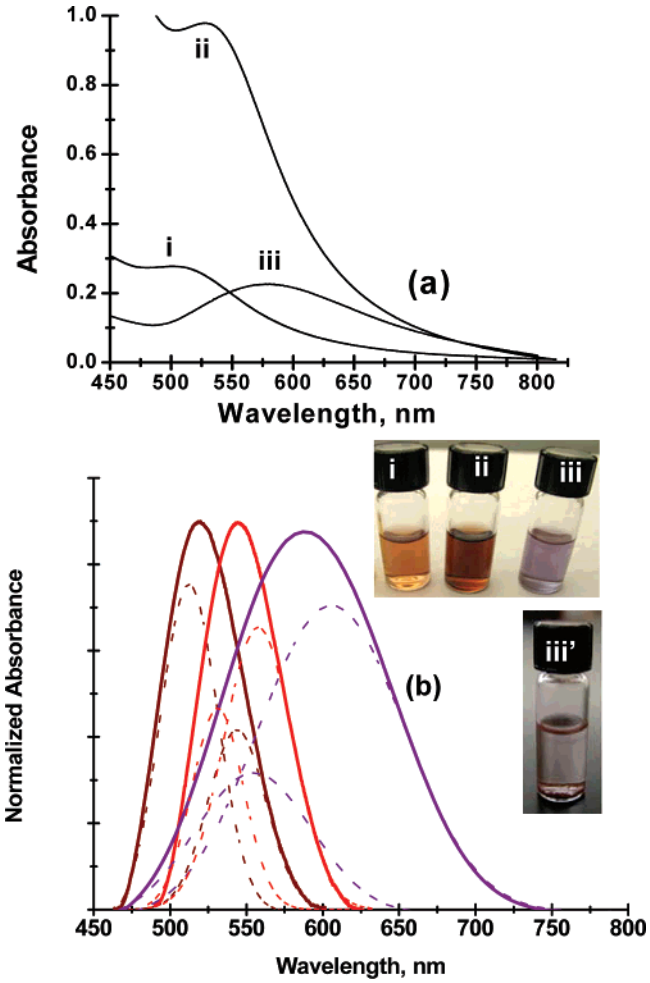

Figure 8. (a) Absorption spectra showing the formation of gold nanopatricles after irradiating the following solutions for 1−2 h: (i) a mixture of 4 mL of 8.0×10^{-5} M (*p*-tosyl)$CH_2NCAuCl$ in dichloromethane and 1 mL of 1 mM DAB-Am-16 in methanol (6.4×10^{-5} M final concentration of (*p*-tosyl)$CH_2NCAuCl$), (ii) a mixture of 4 mL of 8.0×10^{-3} M (*p*-tosyl)$CH_2NCAuCl$ in dichloromethane and 1 mL of 1 mDAB-Am-16 in methanol (6.4×10^{-3} M final concentration of (*p*-tosyl)$CH_2NCAuCl$), and (iii) 8.0×10^{-3} M solution of (*p*-tosyl)$CH_2NCAuCl$ in dichloromethane with no dendrimer added. (b) Normalized plasmon absorption peaks (solid lines) with Gaussian peak-fit analysis (dotted lines) for samples i−iii. Vial iii′ contains dark-grayish metallic gold that precipitates when vial iii is left standing for several hours.

It is interesting to note that the relative long-term stability of the solids and solutions of the compounds examined here is commensurate with their photochemical reactivity. For example, solutions of Au(CO)Cl readily form metallic gold even under room light within an hour. On the other hand, solutions of (*p*-tosyl)$CH_2NCAuCl$ are not extremely light sensitive and remain clear and colorless for several days before they decompose, while the solid compound can be stored in room light only for several weeks before it starts decomposing. In contrast, *t*-BuNCAuCl and MeNCAuCl are extremely stable to light, as we have not observed any decomposition for solids and solutions of both compounds upon extended storage under room light. These observations clearly correlate with the quantum yield (Φ) values shown in Table 3 for the formation of the metallic gold and $LAuCl_3$ photoproducts. Indeed, the trend of the relative

(54) (a) Hoggard, P. E. *Coord. Chem. Rev.* **1997**, *159*, 235. (b) Serafimova, I. M.; Hoggard, P. E. *Inorg. Chim. Acta.* **2002**, *338*, 105.

(55) For representative examples of other Au(I) complexes studied photochemically, see: (a) Foley, J. B.; Bruce, A. E.; Bruce, M. R. M. *J. Am. Chem. Soc.* **1995**, *117*, 9595. (b) Che, C.-M.; Kwong, H.-L.; Poon, C.-K.; Yam, V. W.-W. *J. Chem. Soc., Dalton Trans.* **1990**, 3215. (c) Yam, V. W.-W.; Choi, S. W.-K.; Lo, K. K.-W.; Dung, W.-F.; Kong, R. Y.-C. *J. Chem. Soc., Chem. Commun.* **1994**, 2379. See ref 23b for a comprehensive review.

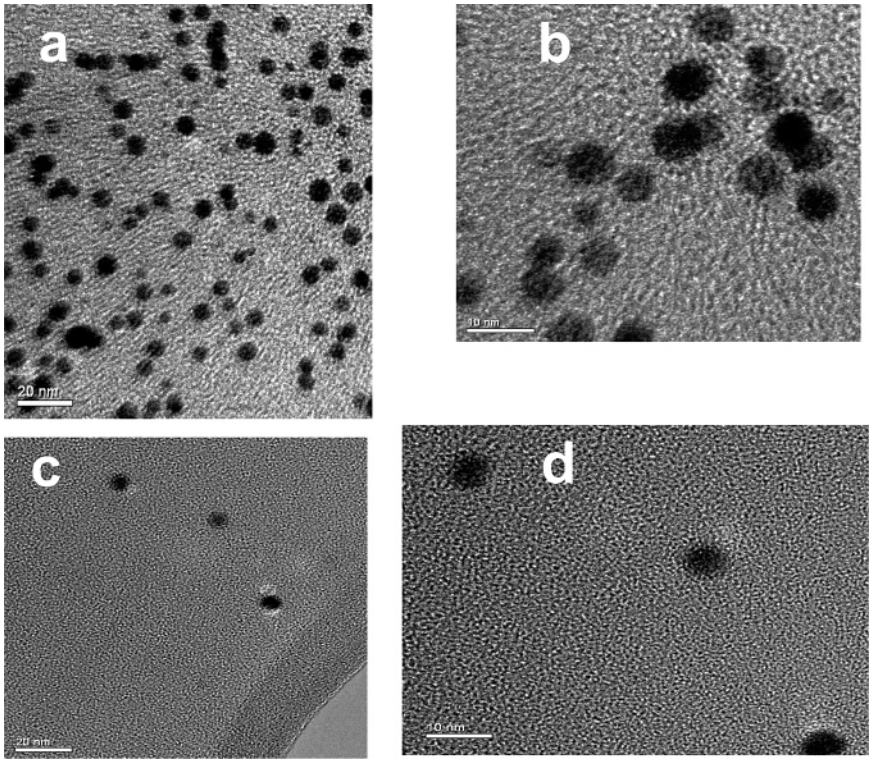

Figure 9. TEM micrographs of dendrimer-stabilized Au nanoparticles using a copper grid covered by carbon film. The particles were prepared by photolysis of 6.4×10^{-3} M (a and b, red solution) and 6.4×10^{-5} M (c and d, brown solution) solutions of (*p*-tosyl)CH_2NCAuCl as described in the caption of Figure 8. Further TEM images are available in the Supporting Information.

long-term light stability based on the π-acceptor ability of L extrapolates to several other LAuX compounds that we have synthesized but have yet to subject to photolysis studies. Thus, we are encouraged to expand the photochemical study herein to investigate the photolysis of multiple other classes of Au(I) complexes which, despite the strong attention given to their photophysical properties, have not been subjected to photochemical studies.[55]

Can the Fundamental Findings Above Aid the Stabilization of Gold Nanoparticles? Since metallic gold is released as a result of the photochemical reactions, it occurred to us to conduct the photolysis reactions in solutions that contain dendrimers terminated with primary amines, which are known to stabilize gold nanopatricles commonly generated via wet chemical reduction of Au(III) precursors.[56] Thus, photolysis of (*p*-tosyl)CH_2NCAuCl solutions that contain the DAB-Am-16 dendrimer leads to solutions that exhibit multiple visible colors depending on the initial concentration of the photoreactant. Figure 8 shows that such colors correspond to broad absorption peaks with $\lambda_{max} = 516$ and 536 nm for two representative photolized solutions with initial (*p*-tosyl)CH_2NCAuCl concentrations of 6.4×10^{-5} and 6.4×10^{-3} M, respectively; see traces i and ii in Figure 8. This result is a clear indication of the formation of gold nanopatricles with different sizes.[35,36,57] The isolated plasmon absorptions of these two photolized solutions give rise to brown and red colors, respectively, representing evenly dispersed suspensions that look clear to the naked eye due to the small particle size. These are contrasted with the purple suspension that results from the photolysis of a 8.0×10^{-3} M solution of (*p*-tosyl)CH_2NCAuCl with no dendrimer stabilizer added. The latter gives rise to a broader and more red-shifted absorption peak ($\lambda_{max} = 590$ nm, trace iii in Figure 8), which is characteristic of surface plasmon absorption of large particles and a large size distribution.[35,36,57] In the absence of dendrimer, the gold nanoparticles agglomerate even further, as evidenced by a clear physical change from a purple evenly dispersed suspension to dark grayish colloids that precipitate after several hours (Figure 8b). In contrast, gold nanoparticle suspensions that contain a stabilizing dendrimer are known to maintain their colors and dispersion stability.[56] This is indeed the case for the gold nanoparticles we have prepared by photolysis of (*p*-tosyl)CH_2NCAuCl solutions that contain the DAB-Am-16 stabilizing dendrimer, for which we have not seen any evidence of agglomeration during the approximately 9-month period since their original preparation and the publication of this manuscript.

Figure 9 shows representative transmission electron microscopy (TEM) images for the gold nanoparticles corresponding to the aforementioned brown and red solutions while more TEM images are provided in the Supporting Information (Figures S3 and S4). These TEM images show well-organized spherical Au nanoparticles with an average particle diameter of 5.3 nm for the brown solution and 6.5 nm for the red solution, as calculated by averaging the particle diameters in selected regions of the TEM images that represent the most dominant particles in each solution. The smaller-sized gold nanoparticles are more monodispersed and have a somewhat more uniform spherical shape in comparison to the larger particles. The particle size increase

(56) For some representative examples, see: (a) Balogh, L.; Valluzzi, R.; Laverdure, K. S.; Gido, S. P.; Hagnauer, G. L.; Tomalia, D. A. *J. Nanopart. Res.* **1999**, *1*, 353. (b) Crooks, R. M.; Zhao, M.; Sun, L.; Chechik, V.; Yeung, L. K. *Acc. Chem. Res.* **2001**, 34, 181. (c) Balogh, L.; Tomalia, D. A. *J. Am. Chem. Soc*. **1998**, *120*, 7355. (d) Garcia, M. E.; Baker, L. A.; Crooks, R. M. *Anal. Chem.* **1999**, *71*, 256. (e) Zhao, M.; Crooks, R. M. *Adv. Mater*. **1999**, *11*, 217.

(57) Link, S.; El-Sayed, M. A. *Int. Rev. Phys. Chem.* **2000**, *19*, 409.

obtained by TEM for the dominant Au nanoparticles in the red versus brown solution is consistent with the observed red shift of the electronic absorption maximum and color change. There are other particles with different sizes seen in the TEM data besides the sizes quoted above (Figures S3 and S4), but the combination of the TEM and spectral data suggest that, in general, the particles are much more uniform in these dendrimer-stabilized samples than the particles formed in the absence of dendrimers. Further data in the Supporting Information (Figures S5−S7) illustrate multi-Gaussian peak fitting analysis for the broad plasmon absorptions resulting from the photolysis of various $LAu^{I}Cl$ complexes, leading to several components sometimes with a very high-energy separation between the peak maxima. The multiple Gaussian peaks for each sample are characteristic of different Au_m particle sizes, which is consistent with our proposed model. The generation of more than one dominant set of Au_m particles and the possible relevance of other mechanisms, as discussed above, are factors that contribute to making the relative quantum yield of $LAuCl_3/Au_m^0$ different from the 1:2 stoichiometric ratio of the disproportionation step in the proposed mechanism.

Finally, we wish to comment on the observation that photochemical changes leading to gold nanoparticle formation are slow initially and increase with further irradiation. The photoinduced production of AuCl leads to incremental formation of gold atoms, which agglomerate to form small metal clusters. The clusters formed can potentially act as nucleation centers that might also catalyze the disproportionation of the remaining AuCl and affect the size variation of the gold nanoparticles. This constitutes autocatalysis by the Au nanoparticles formed from the growth of the nucleation centers.[58] However, further studies are warranted to investigate this effect systematically as has been done in ref 58. Efforts are also ongoing for assessing the suitability of the gold nanoparticles prepared photochemically as described herein for catalytic and biomedical applications.

Acknowledgment. Dedicated to Prof. Hubert Schmidbaur. We thank the National Science Foundation (CAREER Award, Grant CHE-0349313), the Robert A. Welch Foundation (Grant B-1542), and the U.S. Department of Energy (Award DE-FC26-06NT42859) for partial funding of this research. We thank Dr. José Calderón for his extensive assistance with the acquisition of the HPLC data. We also thank Mr. Taehon Lee and Prof. Moon Kim for the acquisition of TEM micrographs at the University of Texas−Dallas.

Supporting Information Available: Further spectral, chromatography, and TEM data referred to in the text above (PDF format). This material is available free of charge via the Internet at http://pubs.acs.org.

JA0703933

(58) Mallick, K.; Wang, Z. L.; Pal, T. *J. Photochem. Photobiol. A* **2001**, *140*, 75.